Measurement of Inherent Deformations in Typical Weld Joints Using Inverse Analysis (Part 2)
Prediction of Welding Distortion of Large Structures†

LIANG Wei*, DENG Dean And MURAKAWA Hidekazu*****

Abstract

During welding, deformation is produced as an unavoidable consequence. The inherent deformation method, in which the inherent deformation is introduced into the elastic FEM as the initial strain is one of the effective methods to predict the welding distortion of large structures. However, the values of the inherent deformations for all weld joints included in the structure must be known before hand. Generally, the inherent deformations are influenced by various factors such as materials, welding method, welding condition, joint geometry, thickness of plate and weld length. Thus, it is meaningful to develop a simple method to obtain the inherent deformation. In this report, a simple and efficient method to estimate inherent deformation of typical weld joints is proposed. Further, using the estimated inherent deformation, the welding deformation of joint specimens and large plate structures are predicted.

KEY WORDS: (*Inherent deformation),(Inverse analysis), (Welding distortion), (Prediction), (Database).*

1. Introduction

Welding is a key technology for building metal structures such ships, bridges, automobiles. However, it is impossible to avoid distortion due to intrinsic nature of the non-uniform heating and cooling of the weldment. Welding deformation not only degrades the performance but also increases the building cost of the structure. It is also an obstacle for realizing automation and robotization. In order to solve these problems, it is necessary to quantitatively predict and control welding deformations.

Generally, welding deformations are classified into transverse shrinkage, angular distortion, rotational in-plane distortion, longitudinal shrinkage, buckling distortion and longitudinal bending distortion as shown in **Fig. 1**. In principle, there are four fundamental types of deformation, namely the longitudinal shrinkage, the transverse shrinkage and the angular distortions in two directions and various forms of distortions are produced as their combination. These four types of deformation can be regarded as fundamental components of the inherent deformations due to welding.

When the welding line is long enough, the distribution of the inherent deformation along the welding line can be assumed to be a constant value [1)], which is mainly determined by the heat input Q, the thickness of the plate h and the type of joint[2)]. As an example, the relationship between angular distortion under the bead on plate welding and the heat input parameter Q/h^2 is shown in **Fig. 2**. As seen from the figure, the inherent deformation can be regarded as a function of the heat input parameter Q/h^2. Once the inherent deformations are given as functions of the heat input parameter, welding deformation of a large welded structure, like the structure shown in **Fig. 3** can be predicted by an elastic finite element method using the concept of inherent deformation[3, 4)]. However, in the welding assembly of thin plates, the short weld whose length is between 20~200 mm is frequently employed. In this situation, the inherent deformation is affected not only by the heat input parameter Q/h^2 but also by the length of the weld Lw.

In this work, the distribution characteristic of the

† Received on July 1, 2005
* Graduate student
** ASTOM Co. Ltd.
*** Professor

Transactions of JWRI is published by Joining and Welding Research Institute of Osaka University, Ibaraki, Osaka 567, Japan.

inherent deformation along the welding line for a weld with a short length is studied. Then a simple measuring method of welding inherent deformation using inverse analysis [5] is proposed. In the inverse analysis, the inherent deformation is estimated from the three-dimensional coordinates at a small number of selected points before and after the welding. Estimated inherent deformations are used to reproduce the welding deformation of the joint specimen or to predict the distortion of large plate structures. The accuracy of the prediction is examined by comparison with experiments.

2. Distribution characteristic of inherent deformation

When the welding line is shorter than the length of the welded plate, the weld length may have a large influence on the inherent deformation. Therefore, the distribution characteristic of inherent deformation along the welding line should be studied first. Generally, for the weldment with a long weld length, two methods can be used to obtain the inherent deformation. One is the experimental method, and the other is numerical simulation using the thermal-elastic-plastic finite element method. In order to obtain the detailed information of inherent deformation and to clarify its distribution characteristic along the welding line for short welds, a thermal-elastic-plastic finite element method is employed in this study.

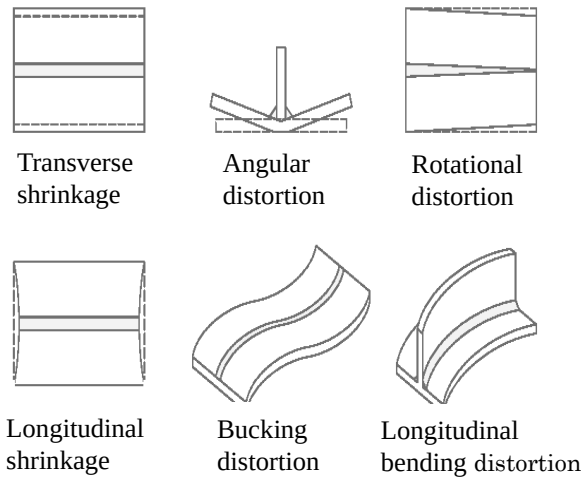

Fig. 1 Types of welding deformation.

The partial bead welding on a flat plate as shown in **Fig. 4** is taken as an example. Half of the model is analyzed due to the symmetry. The dimensions of the model are: L=200 mm, B=100 mm and h=3.0 mm. The heat input parameter Q/h^2 is assumed to be 14.8 J/mm^2. The middle part of the plate is assumed to be welded. The length of the weld is 100 mm in this case. The half plate is uniformly divided into 50 and 4 elements in the welding and the thickness directions. The FEM model consists of 4000 brick elements and 5355 nodes. It has a fine grid in the welding zone. The material of the plate is mild steel, the temperature dependent thermal and mechanical properties are used in the analysis. The problem is solved using ABAQUS employing the "DC3D8" element and "C3D8I" element for thermal and stress analysis, respectively.

The welding distortion is assumed to be caused by four components of inherent deformation, namely longitudinal shrinkage δ^*_x, transverse shrinkage δ^*_y, longitudinal bending θ^*_x and transverse bending θ^*_y. These four components of inherent deformation can be defined by the following equations:

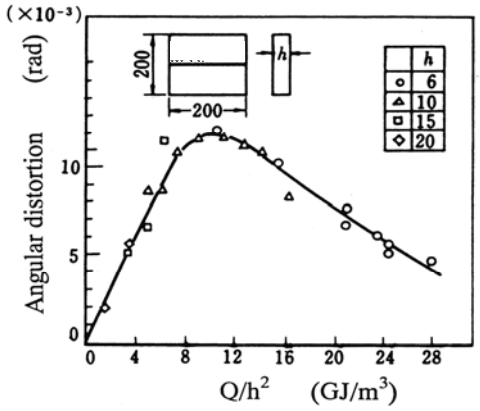

Fig. 2 Relationship between angular distortion and Q/h^2.

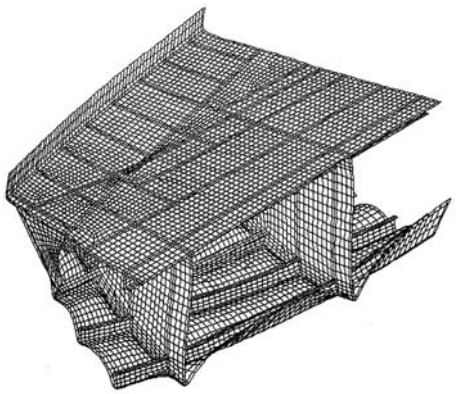

Fig. 3 Welding distortion of ship structure calculated by elastic FEM.

$$\delta^{i}_{x} = \int \varepsilon^{i}_{x} dydz \quad / h$$
$$\delta^{i}_{y} = \int \varepsilon^{i}_{y} dydz \quad / h$$
$$\theta^{i}_{x} = \int \varepsilon^{i}_{x} (z - h / 2) /(h^{3} / 12) dydz \qquad (1)$$
$$\theta^{i}_{y} = \int \varepsilon^{i}_{y} (z - h / 2) /(h^{3} / 12) dydz$$

Where, ε^{i}_{x} is the plastic strain in the welding direction x, ε^{i}_{y} is that in y direction obtained as the results of the thermal-elastic-plastic FEM analysis.

The distributions of the inherent deformation are shown in **Fig. 5**. From these figures, it is seen that the distribution of the inherent deformation is fairly uniform in the middle part of the weld and they can be assumed as constant values without significant loss of accuracy.

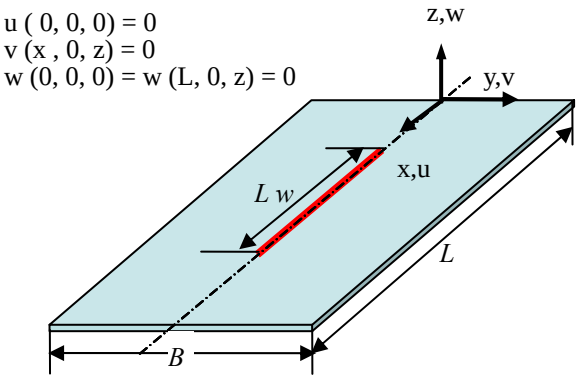

Fig. 4 Bead on plate welding specimen.

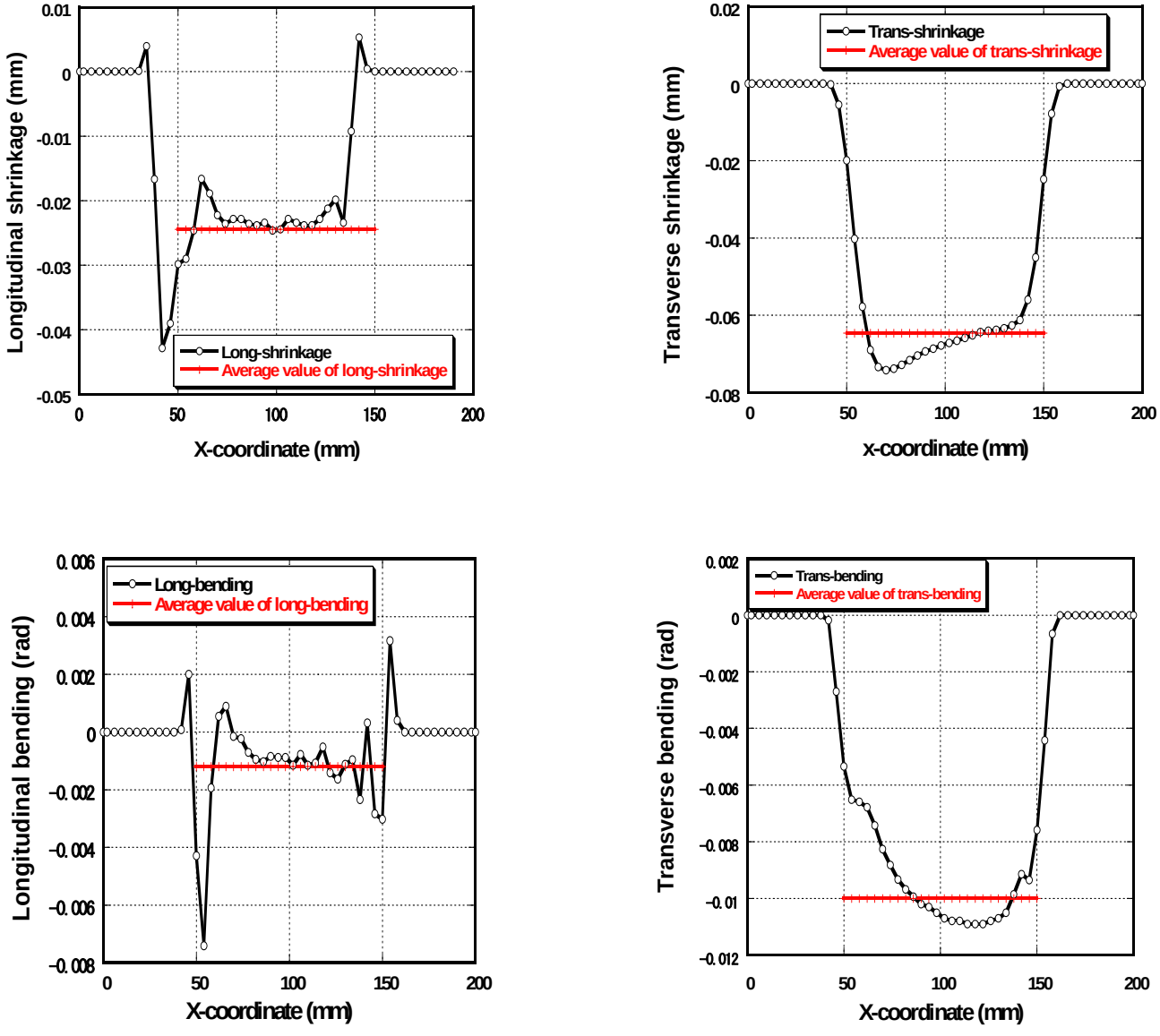

Fig. 5 Distribution of the inherent deformation.

3. Measurement of Inherent Deformation by Inverse Analysis

If the distribution of the welding inherent deformation is expressed in terms of a small number of parameters, the inherent deformation can be determined through inverse analysis based on the measurement of the deformation at limited locations. In this study, a method of inverse analysis is proposed under the following hypotheses:

(1) The four components, namely longitudinal shrinkage, transverse shrinkage, longitudinal bending and transverse bending are regarded as the components of inherent deformations to be determined.

(2) If the distribution function of each component of the inherent deformation is expressed by n parameters, the total number of parameters is $4n$.

(3) The length and the width of the area where the inherent deformation is distributed are known.

(4) The three-dimensional coordinates of m points are measured before and after the welding.

Since the coordinates measured at m points include the rigid body motion, the number of linearly independent relationships is $(3m\text{-}6)$. Thus, the necessary condition for determining the inherent deformation is: $(3m\text{-}6)>4n$.

Based on the above idea, the ten points on the specimen as shown in **Fig. 6** are selected. By measuring the three-dimensional coordinates of the 10 points, the inherent deformation can be determined according to the following procedure:

(1) In order to exclude the rigid body motion, the base triangle is defined. The base triangle consists of points 1, 2 and 3 as shown in **Fig. 6**.

(2) From the coordinates of three vertexes belonging to the base triangle, the stretch of each side gives three independent relations.

(3) Concerning the other measuring points except the points forming the basic triangle, the variations of the distances between each point and the 2 points of the basic triangle give $2(m\text{-}3)$ conditions, similarly, from the variations of the normal distance between each point and the plane defined by the basic triangle, $(m\text{-}3)$ conditions can be obtained.

(4) Adding (2) and (3), the number of the total relations becomes $(3m\text{-}6)$.

(5) The relations defined in (2) and (3) are basically the equations relating the inherent deformation a_i and the deformation of the specimen F^m_j such as the stretch between two points or the deflection relative to the base triangle, i.e.

$$F_j(a_i)=F^m_j \qquad (2)$$

where, a_i: components of inherent deformation

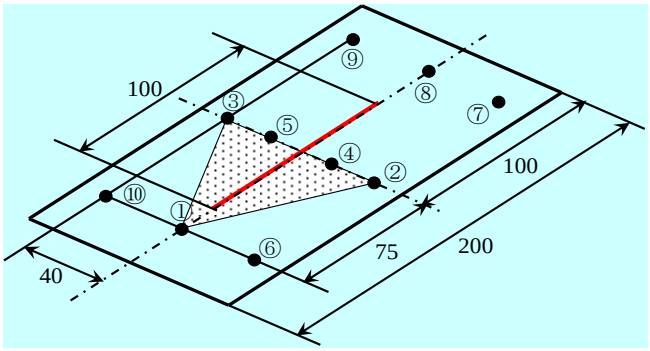

Fig. 6 Measurement points for inverse analysis.

$F_j(a_i)$: deformation which is computed by FEM using inherent deformation a_i

F^m_j: measured deformation

(6) Since the relation between the inherent deformation a_i and the deformation of the specimen $F_j\ (a_i)$ is nonlinear, the function $F_j(a_i)$ is nonlinear. Therefore, the inherent deformation a_i can not be determined from the measured value F^m_j by a single step. It must be determined through an iterative process based on the following Taylor expansion.

$$F_j(a_i+\Delta a_i)=F_j(a_i)+(\partial F_j/\partial a_i)\,\Delta a_i = F^m_j \qquad (3)$$

or in matrix form,

$$[\partial F_j/\partial a_i]\,\{\Delta a_i\}=\{F^m_j - F_j(a_i)\} \qquad (4)$$

where, Δa_i is the correction to the approximate solution at the previous step.

Since Eq. (4) is a set of simultaneous equations consisting of (3m-6) equations which is larger than the number of unknowns $4n$. The unknowns Δa_i can be determined as a least square solution through the following equation.

$$[\partial F_j/\partial a_i]^T\,[\partial F_j/\partial a_i]\,\{\Delta a_i\} = [\partial F_j/\partial a_i]^T\,\{F^m_j - F_j(a_i)\} \qquad (5)$$

4. Inherent Deformations in Simple Weld Joints

Using the coordinates measured before and after the welding, the inherent deformation in three simple weld joints, namely bead on plate welding, lap joint and fillet joint shown in **Fig. 7** are estimated by the inverse analysis described above. The welding conditions for these specimens are shown in **Table 1**. To examine the validity of the estimated inherent deformations, the welding deformation produced by these inherent deformations is computed as a forward analysis and compared with the measured values. As an example of computed results, the distribution of the deflection in bead on plate welding is shown **Fig. 8**. The deformations calculated from the measured coordinates F^m_j and those from the forward analysis $F_j(a_i)$ are compared in **Fig. 9**.

The same plots are shown for the lap joint and the filet joint in **Figs. 10-13**. As seen from **Figs. 9, 11, 13**, the measurement and forward analysis show good agreement. This proves the accuracy of the estimated inherent deformation determined by the proposed inverse analysis.

5. Prediction of Welding Distortion in Large Plate Structures

5.1 Test Models

In order to verify the effectiveness of the proposed method, two experimental models shown in **Fig. 14** are fabricated and their welding distortions are measured. Model A consists of a skin plate and two longitudinal stiffeners, and model B consists of a skin plate, three longitudinal stiffeners and two transverse stiffeners. The thickness of both the skin plate and the transverse stiffener is 9 mm, and that of the longitudinal stiffener is 12 mm. The steel used for the models is SM400A. The welding is done by CO_2 gas metal arc welding using flux-cored wire. In the experiments, effects of gap between skin plate and the longitudinal stiffeners produced by geometrical error of the stiffener on the final welding distortion is also examined. Thus, four experiments, A-1, A-2, B-1 and B-2 are made. In case A-1 and case B-1, all members have no geometrical error, so there is no initial gap. In case A-2 and case B-2, there are initial gaps between the longitudinal stiffeners and the skin plate. The size of the gap is the maximum at both ends and it is approximately 10 mm. As an example, the distributions of the initial gaps in case B-2 are shown schematically in **Fig. 15**.

In case A-1 and case B-1, all members are tack welded at first, then the final welding is performed. In case A-2 and case B-2, the initial gaps are closed by pulling the skin plate to the longitudinal stiffener, then all the members are tack welded and the final welding is done. The welding conditions for Model A and Model B are shown in **Table 2**.

5.2 Determination of inherent deformation

The structure models Model A and Model B are assembled by three types of fillet joints, namely joints between longitudinal stiffener and skin plate (LS-joint), between transverse stiffener and skin plate (TS-joint) and that between longitudinal and transverse stiffeners (LT-joint). The inherent deformations of these three joints are determined by two methods. One is the proposed inverse analysis and the other is thermal-elastic-plastic analysis using ABAQUS.

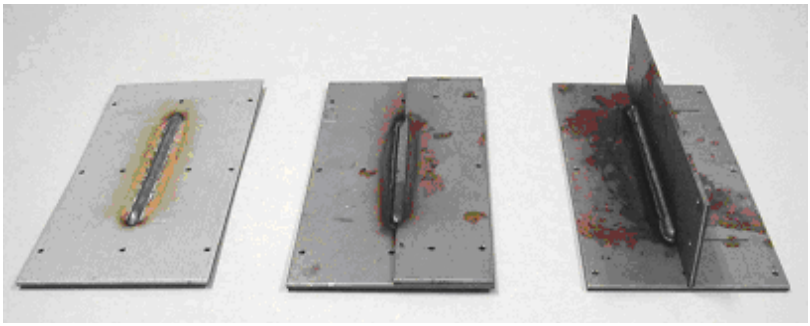

(1) Bead welding. (2) Lap joint. (3) One side T fillet.
Fig. 7 Typical welded joint.

Table 1 Welding parameters of welding experiments.

Weld joint	Welding Parameters			Q/h^2 (J/mm^3)
	Welding Current (A)	Arc Voltage (V)	Welding Speed (mm/s)	
Bead welding	200	20	15	29.6
Lap joint	100	20	10	22.2
Fillet joint	100	10	20	5.6

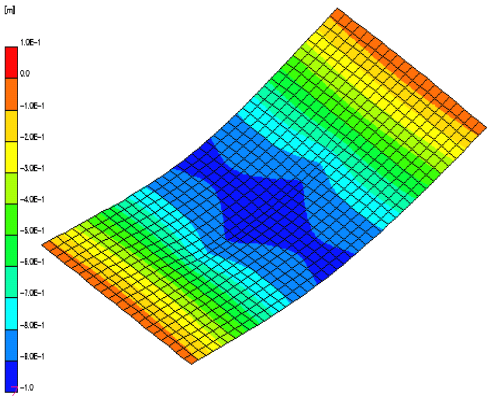

Fig. 8 Predicted deflection of bead on plate.

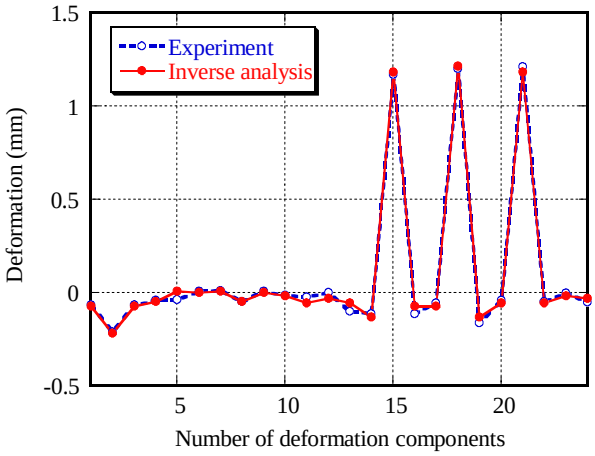

Fig. 9 Comparison of deformation between measurement and forward analysis (bead welding).

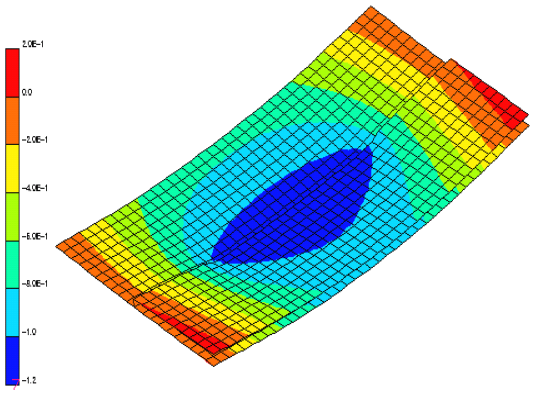

Fig. 10 Predicted deflection of lap joint.

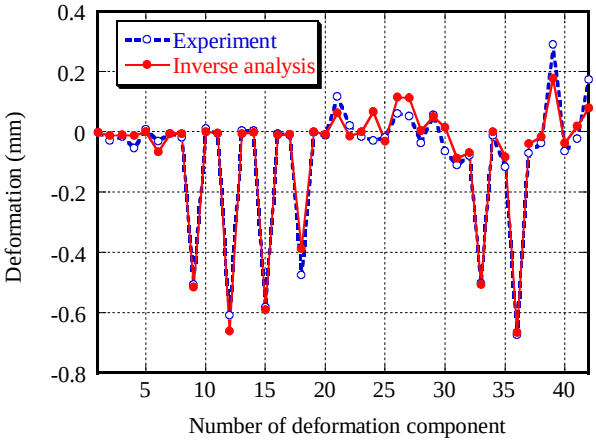

Fig. 11 Comparison of deformation between measurement and forward analysis (lap joint).

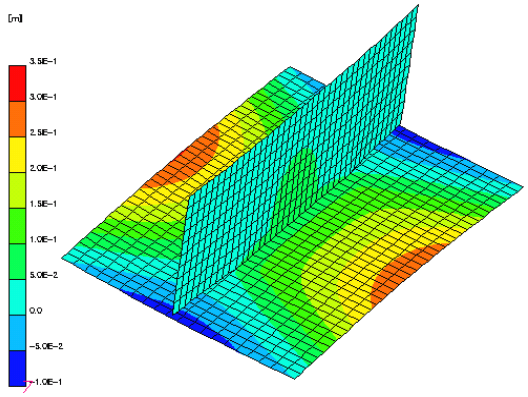

Fig. 12 Predicted deflection of fillet joint.

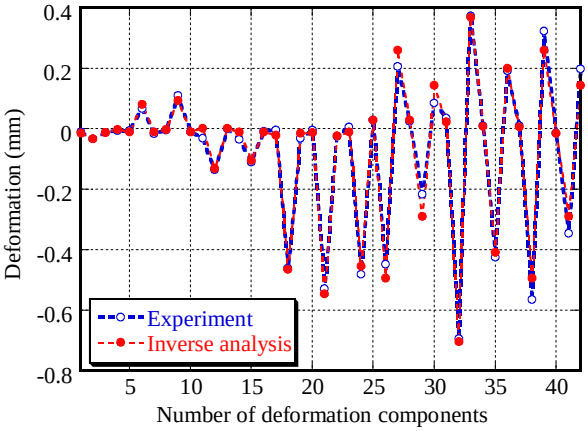

Fig. 13 Comparison of deformation between measurement and forward analysis (fillet joint).

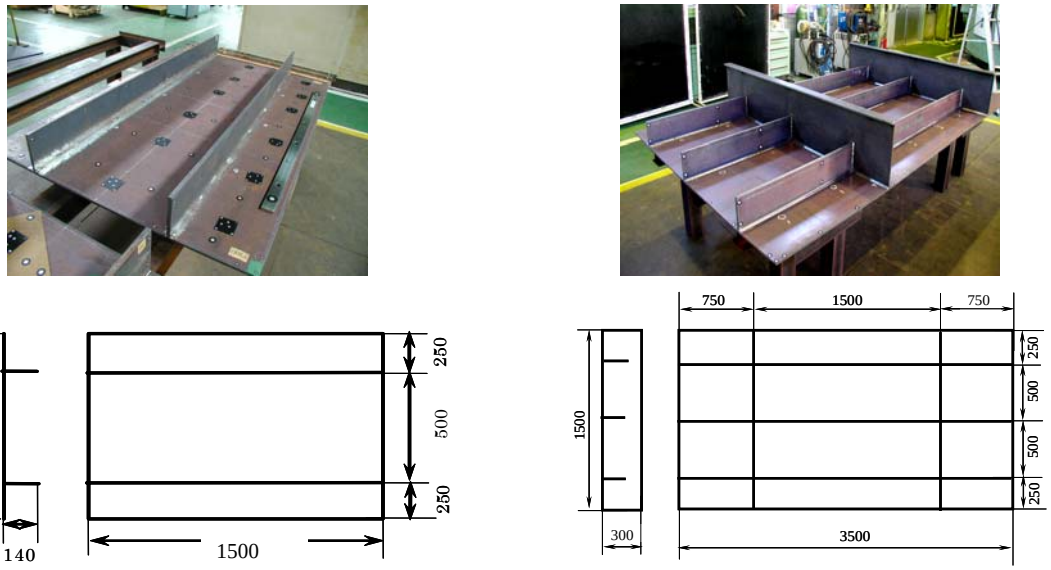

(1) Model A (2) Model B

Fig. 14 Test specimen of model A and model B

Table 2 Welding parameters for three fillet weld joints.

Weld joint	Current (A)	Voltage (V)	Speed (mm/s)	Leg Length (mm)
L-S	270	29	6.67	6
T-S	270	29	6.67	6
L-T	180	21	5.17	6

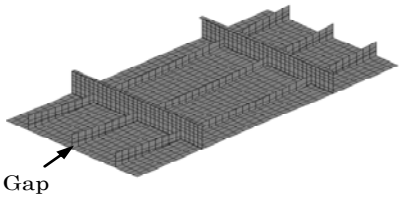

Fig. 15 Initial gap in Model B-2.

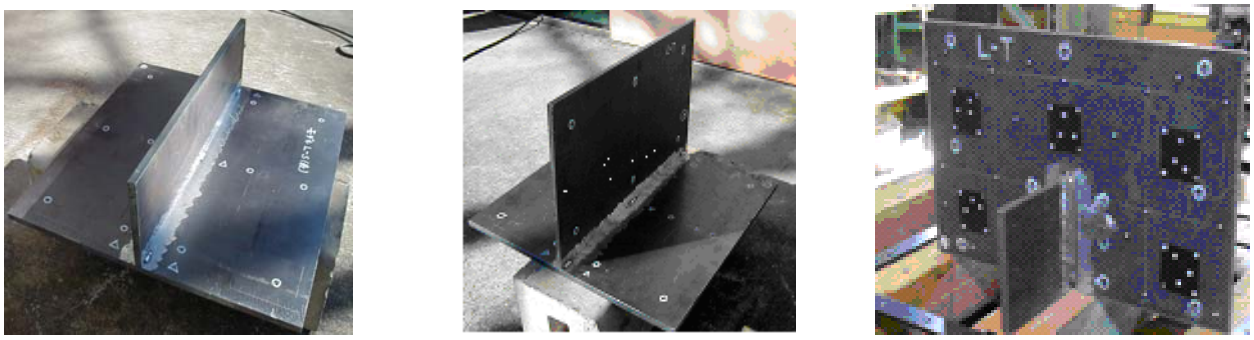

LS-joint TS-joint LT-joint

Fig. 16 Fillet weld joint specimen for estimating inherent deformation.

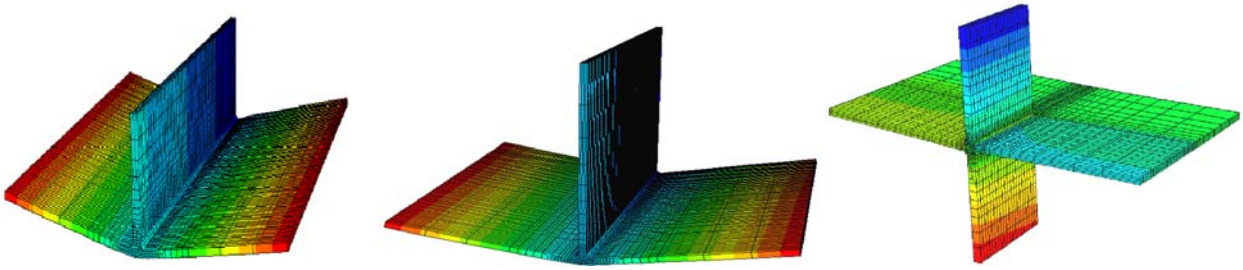

LS-joint TS-joint LT-joint

Fig. 17 Deformation of fillet joints computed using ABAQUS.

Table 3 Inherent deformation of fillet joints.

Model	Method	Welding position	Tendon Force(N)	Transverse shrinkage(mm)	Angular Distortion(rad)
L-S	Inverse Analysis	Skin	260400	0.22	0.0240
		stiffener		-----	-----
	FEM	Skin	222790	0.16	0.0275
		stiffener		-----	-----
T-S	Inverse Analysis	Skin	185470	0.25	0.0266
		stiffener		-----	-------
	FEM	Skin	192418	0.215	0.0260
		stiffener		-----	-----
L-T	Inverse Analysis	----------			
	FEM	Skin	189470	0.25	0.004
		stiffener		0.165	0.003

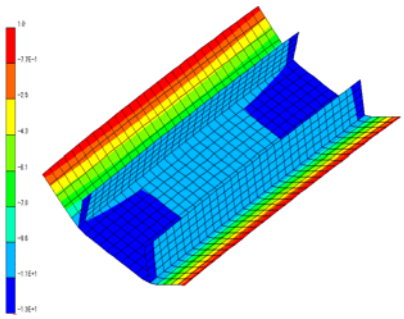

(a) Model A-1

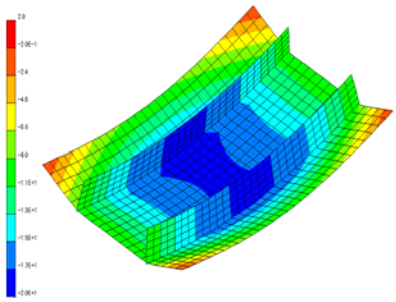

(b) Model A-2

Fig. 18 Predicted deflection.

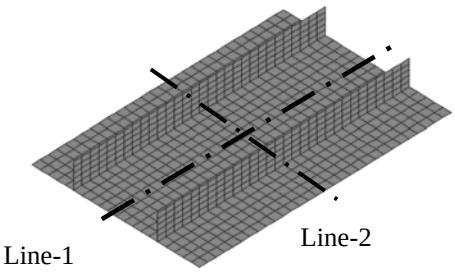

Fig. 19 Lines for comparison.

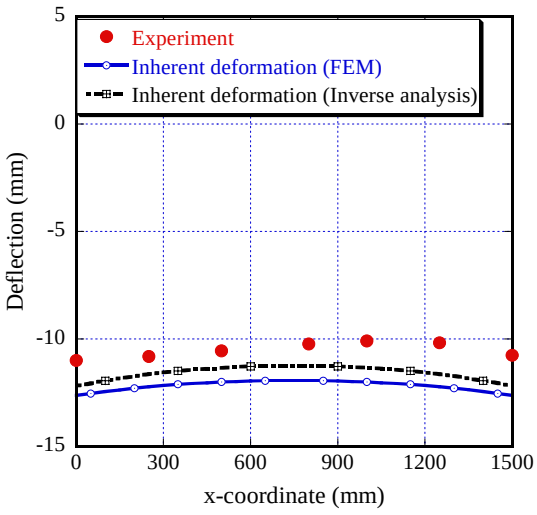

(a) along Line-1

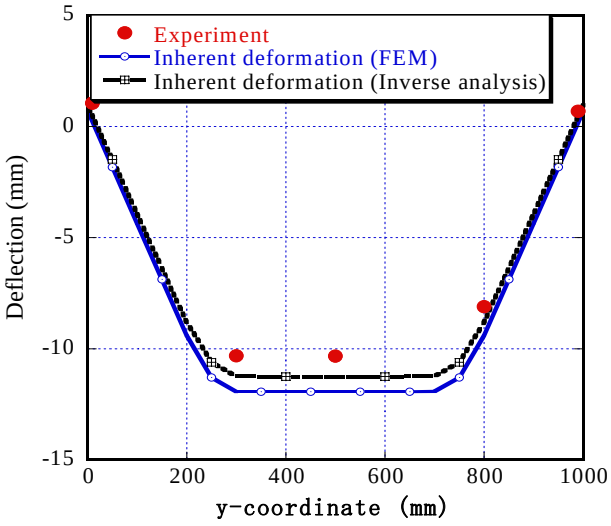

(b) along Line-2

Fig. 20 Comparison of deflection between experiments and prediction using inherent deformation.

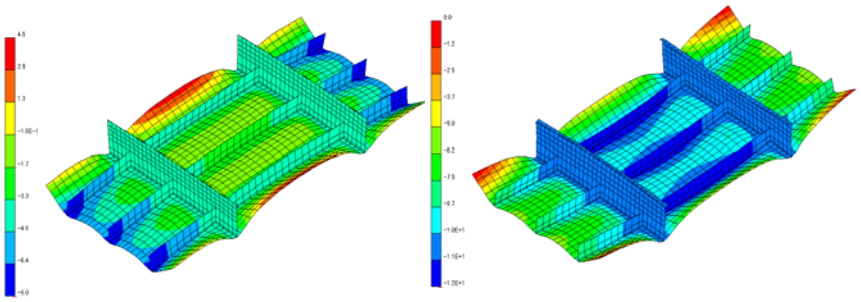

(a) Model A-1 (b) Model A-2

Fig. 21 Predicted deflection.

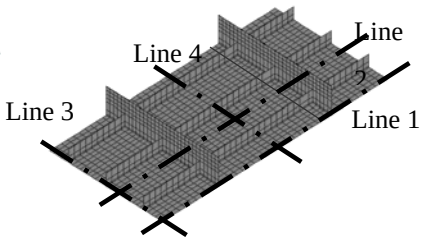

Fig. 22 Lines for comparison.

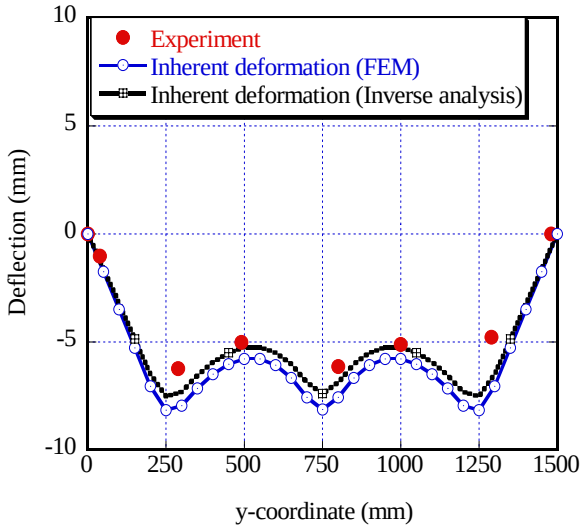

Fig. 23 Comparison of deflection along Line-3 between experiment and prediction(Model B-1).

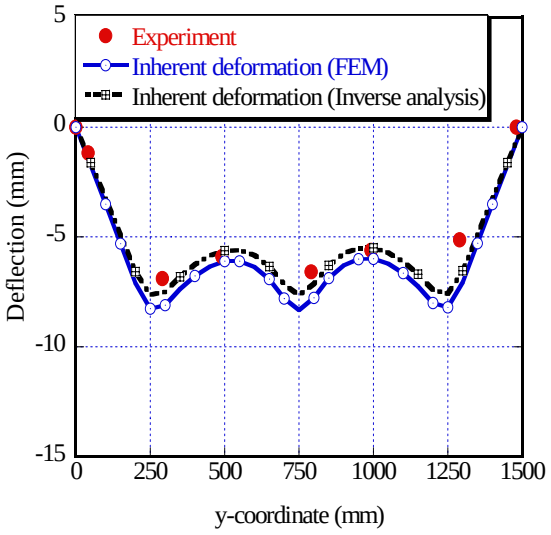

Fig. 24 Comparison of deflection along Line-3 between experiment and prediction (Model B-2).

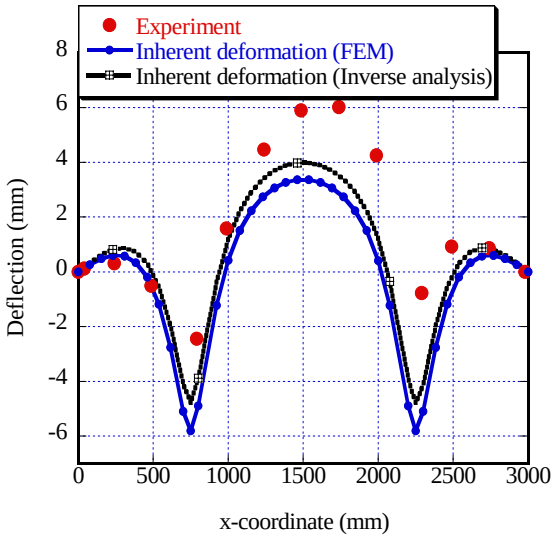

Fig. 25 Comparison of deflection along Line-2 between experiment and prediction (Model B-1).

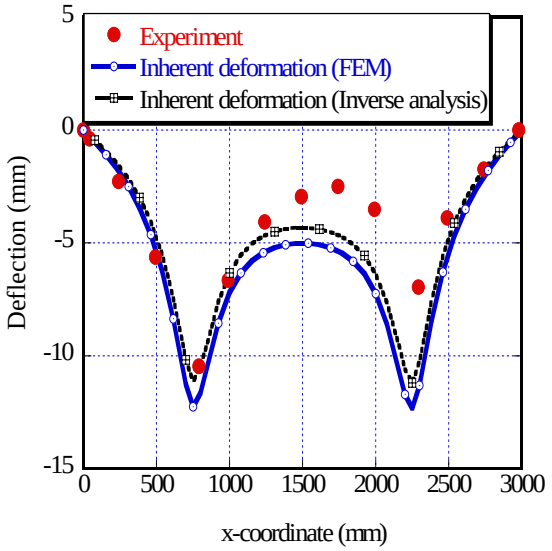

Fig. 26 Comparison of deflection along Line-2 between experiment and prediction (Model B-2).

Three joint models, namely LS-joint, TS-joint and LT-joint shown in **Fig. 16**, are made. The inherent deformations are determined from three-dimensional coordinates measured before and after welding using inverse analysis. The welding deformations computed for the same joints by the thermal-elastic-plastic FEM are shown in **Fig. 17**. The inherent deformations estimated using the two methods are summarized in **Table 3**. Though the convergence in the inverse analysis is not reached for the LT-joint due to the poor accuracy of the coordinate measurements, generally good correlation is observed between the inherent deformations estimated by two methods.

5.3 Predicted deformation of model A

Using the inherent deformation shown in **Table 3**, the welding deformations of Model A-1 and A-2 are predicted by the inherent deformation method. **Fig. 18** shows the vertical deflections of the models A-1 and A-2. For the quantitative comparison, the deflections along Line-1 and Line-2 defined in **Fig. 19** are plotted. **Fig. 20** shows the deflection along Line-1 and Line-2. The welding deformations predicted using the inherent deformations estimated by the thermal-elastic-plastic FEM and the inverse analysis coincide fairly well with each other. The difference is about 1 mm. The deflections measured by experiment are plotted as solid circles. The deflection predicted using the inherent deformation estimated by the inverse analysis is closer to the experiments compared to that by thermal-elastic-plastic FEM. This proves that the inherent deformation estimated by the inverse analysis can be used to predict the welding deformation of Model A with reasonable accuracy.

5.4 Predicted deformation of model B

The welding distortions of Model B are also predicted in the same manner as in the case of Model A. **Fig. 21** shows the vertical deflections of the models B-1 and B-2. For the quantitative comparison, the deflections along Line-3 and Line-2 defined in **Fig. 22** are plotted. **Fig. 23** and 24 show the deflections along Line-3 in Model B-1 and Model B-2. As in the case of Model A-1, the welding deformations predicted using the inherent deformations estimated by the thermal-elastic-plastic FEM and the inverse analysis coincide fairly well with each other. The difference is approximately 1 mm. The deflections measured by experiment are plotted as solid circles. As seen from the figures, the predicted deflections along Line-3 agree very well with the experiment.

Similarly, the deflections along Line-2 are plotted in **Figs. 25-26**. The deference between the two predicted deflections is small. Though the agreement between the predictions and the measurement is generally good, relatively large discrepancy is observed in the area $1200 < x < 2500$ mm. Also the measured deflections show unsymmetrical distribution whereas the predicted deflections are symmetric from the symmetry of the problem. Except for this, the inherent deformation method gives reasonable prediction. Comparing the two methods for estimating the inherent deformation, the proposed inverse analysis results in a better prediction.

6. Conclusions

The distribution of the inherent deformation for the partial bead on plate welding is clarified using the thermal-elastic-plastic FEM analysis. Based on this knowledge, a simple method to estimate the inherent deformation by inverse analysis is proposed and applied to compute deformations of typical weld joints and large plate structures. Through the present work the following conclusions are drawn.

(1) Though the values of the inherent deformations vary along the welding line in the partial welding as in the case of full welding, their variations are small in the middle part.

(2) The distribution of inherent deformation can be approximated by uniformly distributed shrinkage and bending in the longitudinal and transverse directions.

(3) The inherent deformations of three typical weld joints, namely bead welding, lap joint and fillet join, are estimated using the inverse analysis and the welding deformations of joints are reproduced through forward analysis with sufficient accuracy.

(4) The proposed inverse analysis is applied to estimate the inherent deformations of fillet joints in large plate structures and the welding deformation of the structures are predicted using the estimated inherent deformations.

(5) Good agreements between the predicted and measured deformations prove that the inherent deformation method employing the inverse analysis is an effective method to predict welding deformations of large welded plate structures.

Acknowledgement

This research is the results of “Development of Highly Efficient and Reliable Welding Technology”, which is

supported by the New Energy and Industrial Technology Development Organization (NODE) through the Japan Space Utilization Promotion Center (JSUP) in the program of Ministry of Economy, Trade and Industry.

References

1) Yu Luo, Hidekazu Murakawa, Morinobu Ishiyama. “Study on Welding Deformation of Plate with Longitudinal Curvature”, Proceedings of Symposium of Welding structure, pp.311-317 (1999).
2) Kunihiko Satoh and Toshio Terasaki. “Effect of welding condition on welding Deformation in welded structural Materials”, Journal of the Japan Welding Society, Vol.45, pp.302-308, (1976)
3) Dean Deng, Hisashi Serizawa and Hidekazu Murakawa. “Theoretical Prediction of Welding distortion in Thin Curved Structure During Assembly Considering Gap and Misalignment”, Symposium of welding structure, pp.129-136 (2002).
4) Dean Deng, Hidekazu Murakawa and Yukio Ueda, Theoretical Prediction of welding Distortion Considering Positioning and Gap Between Parts, International Journal of Offshore and Polar Engineering, Vol.14.No.2, pp.138-144, (2004).
5) Wei LIANG, Shinji SONE, Motohiko TEJIMA, Hisashi SERIZAWA and Hidekazu Murakawa. Measurement of Inherent Deformation in Typical Weld Joints Using Inverse Analysis (Part 1) Inherent Deformation of Bead on Welding, Transactions of JWRI, Vol.33, No.1, pp.45-51, (2004).